A Miniaturized Low-Profile Multi-Layer Frequency Selective Surface Insensitive to Surrounding Dielectric Materials

Muaad Hussein, *Student member, IEEE*, Jiafeng Zhou, Yi Huang, *Senior member, IEEE*, Muayad Kod, Abed Pour Sohrab, *Student member, IEEE*

***Abstract*— In most applications, a Frequency Selective Surface (FSS) needs to be attached to a wide variety of dielectric materials. The performance of a traditional FSS is greatly influenced by the dielectric material to which it is attached. In this paper, a novel multi-layer structure is proposed to construct an FSS. The performance of the proposed structure is shown to be very stable when it is attached directly to a wide variety of dielectric materials of arbitrary thickness. Both single and dual polarized structures are designed. The shape of the FSS element is designed by using stepped-impedance transmission lines. A new methodology is proposed to design the FSS by maximizing the value of the capacitance between adjacent layers. The proposed structure offers three distinctive advantages. Firstly, the strong cross-layer capacitance makes the FSS element very compact. The dimensions of the miniaturized element are as small as $0.012\lambda \times 0.012\lambda$. Secondly, for the proposed structure, the lower the profile, the stronger the cross-layer capacitance, and the lower the resonant frequency. This is unique to the proposed structure since the resonant frequency is usually higher for a lower profile for traditional structures. Thirdly and most importantly, any external dielectric material attached to the FSS will not significantly affect the performance of the FSS due to this strong cross-layer capacitance. Through examples of a single polarized bandpass FSS at 1 GHz and a dual polarized bandpass FSS at 1.96 GHz, it is demonstrated that a stable resonant frequency under various incident angles up to 75º can be achieved.**

***Index Terms*—Frequency selective surface (FSS), multi-layer, radio frequency-identification (RFID), radomes, spatial filters.**

I. Introduction

FREQUENCY Selective Surfaces (FSSs) are periodical structures with an arbitrary shape, generally embedded in or supported by a dielectric substrate. FSSs are essentially resonant periodic arrays which exhibit selectivity in frequency, polarization and incident angle. The use of FSSs has contributed to the ever-increasing communication capabilities of satellite platforms [1]-[4]. They are used in modern military platforms such as aircraft, ships and missiles. FSSs are widely used with antennas and radars to achieve cross section reduction. FSSs can be used in many applications in the civil sector as well, such as isolation of unwanted and harmful radiation in L-band and S-band in hospitals, schools and domestic environments. FSSs have been the subject of intense investigations on a large scale as spatial microwave and optical filters for decades [5]-[12]. Bandstop FSS structures are successfully used to decrease the electrical power in antennas and improve the radiation power [12]. Most antennas act as efficient radiators at the frequency band in which they are designed to operate in and also outside their desired operating frequency range. In such applications, the RCS of the antenna can be reduced to protect it from the outdoor environment and undesired frequencies by using a bandpass FSS. The bandpass FSS is transparent within the antenna's operating frequency and opaque at other frequencies.

FSSs can be classified as the patch type and the mesh type [13]. If the metal patches are not connected, it is called a capacitive surface, and The FSS reflects high frequencies while transmitting low frequencies. On the other hand, the complementary structure is called an inductive surface, and it reflects low frequencies while transmitting high frequencies.

Recently, there has been an interest in the design of FSSs with array element dimensions that are much smaller than the wavelength. The miniaturization of FSS elements is desired to enable an FSS with sufficient number of elements to present as an infinite array because practical FSSs are fabricated in finite dimensions. The miniaturization of an FSS is mainly achieved by increasing the values of resonant elements. An FSS array element can be much smaller than the wavelength at the resonant frequency by adding meander-slots to a circular ring structure in [14]. The creation of a miniature FSS by printing micro wires on a dielectric has been demonstrated in [15]. Using four symmetrical spiral patterns of metallic meander lines can increase the electrical length of the array element and increase the values of resonant components [16]. Two layers, metallic patches and wire meshes, separated by a dielectric substrate were used to miniaturize the array elements in [17], [18]. An FSS element miniaturized by using lumped components has been presented in [19]. Another approach was adopted in [20] by cascading interdigitated capacitors on a thin

Manuscript received June 30, 2016; revised October 19, 2016; accepted May 14, 2017.

The authors are with the Department of Electrical Engineering and Electronics, The University of Liverpool, UK. (e-mail:Jiafeng.Zhou@liverpool.ac.uk).

substrate layer. By cascading a square-loop slot with a periodic array of metallic patches, a compact FSS is implemented on an ultra-thin dielectric layer in [21].

Most FSSs reported in the literature suffer from practical design issues, namely sensitivity to polarization or incident angles, the dimension issue, or the sensitivity when attached to a wide variety of dielectric materials of arbitrary thicknesses. These limitations can restrict the use of an FSS in many applications. For example, the FSSs can be used in radio frequency-identification (RFID) tag applications [22]. A tag is usually attached directly to an object that needs to be identified. Many common materials have very strong effect on the performance of the tag antenna and can shift the resonant frequency significantly. In the worst case, the tag may be unreadable at normal ranges, which would cause tracking systems to miss objects, and vitiate many of the advantages of tags [23], [24]. In some applications, the FSSs need to be attached to dielectric materials for mechanical reasons to make the structure stronger.

This paper describes both a single and a dual polarized FSS structures. Firstly, a two-metallic-layer bandpass FSS element is designed by using a step-impedance structure with very high and very low characteristic impedance transmission lines in each layer. The proposed array element has both meshes and patches. An unconventional methodology is used to miniaturize the FSS element's dimensions. The dimensions of the periodic array element are much smaller than the wavelength at the resonant frequency. The overall profiles (thicknesses) of the multi-layer FSS elements presented in this paper are extremely small. For example, the thickness of the FSS structure consisting of two metallic layers and one dielectric layer is less than 0.15 mm. The proposed structure is designed to exhibit a stable frequency response when it is attached to a wide variety of dielectric materials of arbitrary thicknesses. These features of the proposed structure can make it a very good solution for many applications. In this paper, section II describes the design of a single polarized FSS array element and the approaches to miniaturize the element. The design of a dual polarized FSS array element is explained Section III. Section IV discusses the stability of the FSS array against surrounding dielectric materials. Section V describes the measurement setup and experimental results to verify the theory. Conclusions are finally given in Section VI.

II. Single Polarized FSS Element

Fig. 1 shows the structure of the proposed single polarized FSS element, consisting of two metallic layers separated by a substrate layer. Each metallic layer is printed on one side of the dielectric substrate consisting of an inductive loop with a width of w and two capacitive patches, each with an area of $b \times a$. Numerical analysis of the proposed element was performed by using CST Microwave Studio, using unit cell boundary conditions to provide periodicity along the x and y axes. The FSS is excited by an electromagnetic wave with the propagation vector (**k**) towards the z axis, magnetic field vector (**H**) towards the x axis and electric field vector (**E**) towards the y axis direction. The top and bottom layers are the same, but flipped in the xy plane. In this way, the currents enter and exit from the top layer patches in opposite directions to the bottom layer patches, as shown in Fig. 2. This causes the charges to be distributed in different polarizations between the top and the bottom layers of the FSS, which induces a strong cross-layer capacitor, C_{cc}.

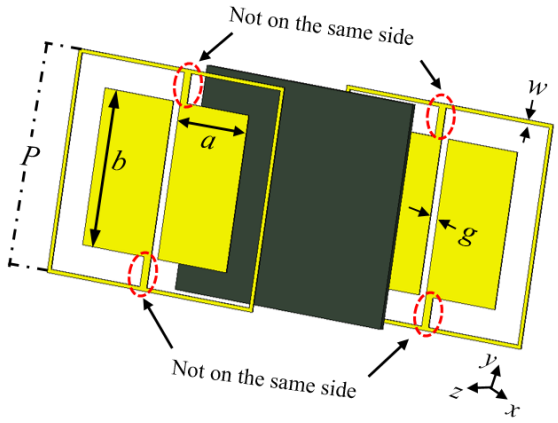

Fig. 1. Array element geometry of the proposed single polarized FSS.

For instance, when an external electrical field, **E**, is applied in the y-axis direction, the current will flow into the left patch and out from the right patch towards the ($-y$) axis direction on the top layer, as shown in Fig. 2(a). This can induce positive charges on the left patch of the proposed element and negative charges on the right one. On the other hand, in the bottom layer, since the structure is flipped, the current will flow into the right patch and out from the left patch towards the ($-y$) axis direction, as shown in Fig. 2(b). This can induce charges opposite to the top layer. Thus, there is a strong cross-layer capacitance existing between the top and the bottom layer. This capacitance offers significant advantages to the FSS element by making the structure compact, low-profile (the lower the profile, the stronger the capacitance) and insensitive to surrounding dielectric materials, as discussed in the following sections.

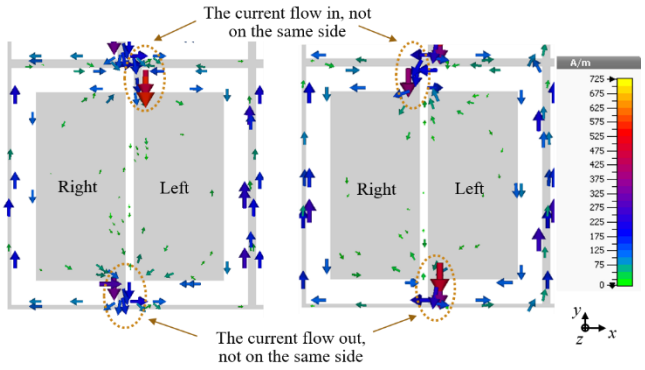

(a) (b)

Fig. 2. Current distribution of the proposed element on (a) the top layer, and (b) the bottom layer.

The proposed structure is designed on an FR4 PCB. The two metallic layers are etched on the top and bottom copper layers of a 0.127 mm-thick FR4 substrate with a dielectric constant of 4.3 and a loss tangent of 0.025. The length of the square patch a is 2.2 mm and the width b is 4.6 mm, the gap width g is 0.2

mm and the width, *w*, of the short line connecting the patches and the loop is 0.1 mm. The periodic constant *P* of the array is 6 mm. Fig. 3 shows the simulated transmission and reflection coefficients. The resonant frequency is 1 GHz with a fractional bandwidth of 6.1%. The reflection coefficient is -19 dB and the insertion loss is 1.13 dB at the resonant frequency. The size of the array element is found to be $0.02\lambda \times 0.02\lambda$**.** The equivalent circuit model of the proposed array element for vertical polarized incident waves is shown in Fig. 4. It should be noted that the circuit model is only used to give a better qualitative understanding of the proposed structure. The actual equivalent circuit is much more complicated than this circuit model. The circuit model consists of an L_1C_1 circuit for the top layer structure, an L_2C_2 for the bottom layer structure and a cross-layer capacitor C_{cc} between them. The substrate between the two metallic layers acts as a transmission line of length *h* (*h* is the substrate thickness) and a characteristic impedance of *Z*. The transmission line is used here as a short circuit because *h* is very small. For example, at the resonant frequency 1 GHz, *h* is $\lambda/2362$. In the circuit model, L_1 is equal to L_2 and C_1 is equal to C_2 due to symmetry.

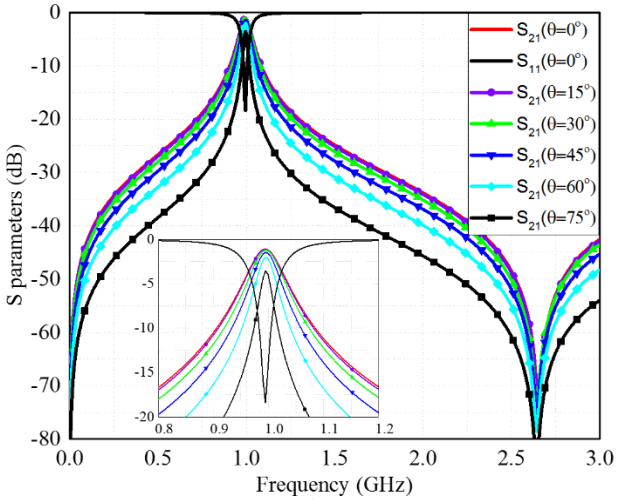

Fig. 3. Simulated frequency response of the proposed two-layer FSS under variable incident angles for the vertical polarization.

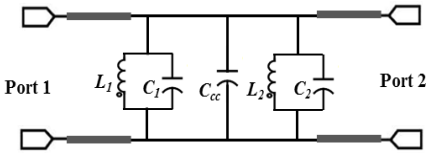

Fig. 4. Equivalent circuit of a two-metallic-layer structure.

The cross-layer capacitance is much stronger than the intrinsic capacitance between the two adjacent patches of each layer. Any dielectric materials attached to the FSS will mainly affect the intrinsic capacitance, but not the cross-layer capacitance. Hence the performance of the proposed FSS is very insensitive to surrounding materials. This advantage will be further discussed in Section IV.

In this case, the circuit model of the FSS element is composed of the parallel *LC* circuits of two metallic layers and the cross-layer capacitor. This means that increasing the number of layers will miniaturize the structure further, although this will be accompanied with bandwidth and insertion loss penalties. The approximate values of the intrinsic inductance and capacitance for TE incident waves can be calculated from the strip inductance and path capacitance using equations in [25],

$$L = \mu_o \mu_e \frac{P}{2n\pi} \log\left[\sin\left(\frac{\pi w}{2P}\right)^{-1}\right] \tag{1}$$

where *L* is the strip inductance, which is determined by the strip length *P*, the strip width *w* and the effective magnetic permeability μ_e of the structure, *n* is the number of metal layers. And

$$C = n\varepsilon_o \varepsilon_e \frac{2b}{\pi} \log\left[\sin\left(\frac{\pi g}{2b}\right)^{-1}\right] \tag{2}$$

where *C* is the intrinsic capacitance between the two adjacent patches in each layer, which is determined by the patch length *b*, the gap *g* between adjacent patches and the effective dielectric constant ε_e of the structure. While the cross-layer capacitance C_{cc} is calculated by using the parallel plates' capacitance equation:

$$C_{cc} = (n-1)\frac{\varepsilon_r \varepsilon_o \mathrm{A}}{d} \tag{3}$$

The overlapping area of the conducting patch is *A* and equal to $2(a \times b)$; the parallel conducting layers are separated by a distance *d*, which is the thickness of the substrate *h* in this case, and the dielectric constant of the substrate is ε_r. It is quite obvious that the cross-layer capacitance is much higher than the intrinsic capacitance of each layer. The approximate theoretical values for the resonator components are $L_1 = L_2 = 3.54$ nH, $C_1 = C_2 = 0.288$ pF, while the value of $C_{cc} = 6.25$ pF. The value of C_{cc} is much greater as expected. The cross-coupling capacitance C_{cc} will significantly lower the resonant frequency of the FSS array element, which makes the element much more compact.

Multi-layer structures are usually used for the design of multi-band or wideband bandpass filters. It can be seen from (3) that the multi-layer structure can also be used to miniaturize the array element. It can be calculated from the equivalent circuit in Fig. 4 that a multi-layer structure is much less sensitive to surrounding materials to be further discussed below.

The cross-layer capacitance is higher with a thinner substrate (lower profile). This is on the contrary of the intrinsic capacitance. The intrinsic capacitance depends on the effective permittivity of the substrate. The effective permittivity is a function of the thickness of the substrate. If the thickness is comparable with the gap width, the effective permittivity is lower with a thinner substrate. The intrinsic capacitance is lower accordingly. If the substrate thickness is much greater than the gap width, the effective permittivity is almost constant. Therefore, the proposed FSS with a lower profile is actually more compact, which is different from traditional structures.

Fig. 5 shows the structure with *n* metallic layers and (*n*-1) dielectric layers. The two transparent layers are only used to

mechanically support assembling the multiple layers together if needed. There are alternative ways of doing this. For example, the layers can be thermally compressed together using a bonding film with a very thin thickness between them [26]. Fig. 6 shows the equivalent circuit of an *n*-layer FSS structure after neglecting the intrinsic capacitance of each metallic layer.

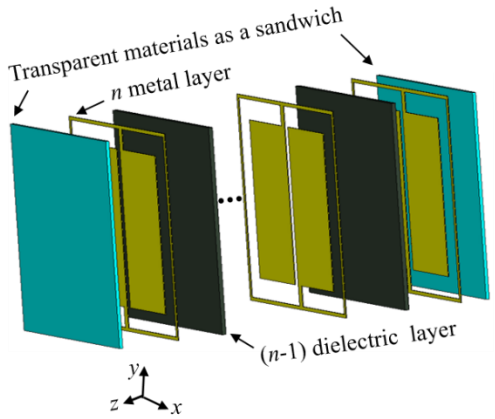

Fig. 5. Array element of the proposed n-metallic-layers FSS with thin dielectric supporters.

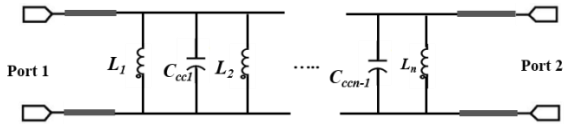

Fig. 6. Equivalent circuit of the proposed n-metallic-layer FSS.

The simulated resonant frequency *f*, fractional bandwidth BW, lowest values of reflection coefficients S_{11} of a multi-layer FSS using the proposed design are summarized in Table I. The periodic dimension *P* is 6 mm, the same for all of these multi-layer structures. It shows that the increase of the number of layers *n* shifts the resonant frequency downward. For example, for *n* = 3 with two FR4 dielectric layers with a thickness of 0.127 mm for each, the resonant frequency is shifted downward to 0.76 GHz from 1 GHz for *n* = 2. The reflection coefficient is -16.9 dB and the fractional bandwidth is 4.62%, as shown in Fig. 7. The FSS array element dimensions in this case are 0.0152λ by 0.0152λ. While using five metallic layers (*n* = 5) and four dielectric layers, the resonant frequency is shifted to 0.6 GHz. The fractional bandwidth is 2.44%, and the reflection coefficient S_{11} is -9 dB. For this case, the size of the element is 0.012λ by 0.012λ.

Table I
Element size vs the number of metallic layers of single polarized FSSs

n	*f* (GHz)	BW	S_{11} (dB)	Over all thickness (mm)	Element size
2	1	6.23%	-19	0.147	0.02λ
3	0.76	4.62%	-14.5	0.284	0.0152λ
4	0.65	3.42%	-13	0.421	0.013λ
5	0.60	2.44%	-9	0.558	0.012λ

To demonstrate the resonant stability performance of the proposed design, the structures of *n* = 2 and *n* = 3 are simulated with variable incident angles, respectively. The proposed structures are insensitive to the angle of incidence (θ) up to 60° for vertical polarizations as shown in Fig. 3 and Fig. 7, respectively.

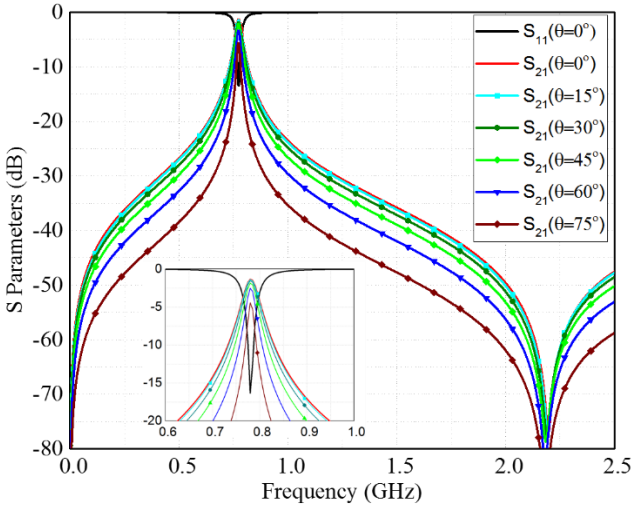

Fig. 7. Frequency response of the proposed three-layer FSS under variable incident angles for the vertical polarization.

III. DUAL POLARIZED FSS ELEMENTS

The FSS element proposed in last section is suitable for single polarized incident waves. The performance of the structure is different if the **E**-field of the incident wave is along the *x*-axis. To achieve dual-polarized performance, the proposed structure can be modified to the one shown in Fig. 8. This structure can be used for not only dual-polarization but also a greater fractional bandwidth. Here, the metallic structure on each layer is 90˚ rotationally symmetrical in the *xy* plane, so that the structure will achieve the same performance if the E-field of the incident wave is either in the *x*-axis or the *y*-axis direction. In the same way as before, the top and bottom layers are the same but flipped in the *xy* plane. Similarly, the dominant capacitor is the cross-layer C_{cc}, compared with the intrinsic capacitor. But the dimension of *b* is halved, which means the value of the capacitance is also about halved. The patch area is a^2 since *b* = 2*a*. This is because only two pairs of patches will have a strong capacitance and the other two patches have relatively weak capacitance depending on the polarization. For example, at vertical polarization, the two patches with strips along *y*-axis in each layer have a strong capacitance to the two patches on the other layer; while other two pairs of patches have weak capacitance. On the other hand, at horizontal polarization, only the patches with strips along the *x*-axis have strong capacitance.

The dual polarized structure has a narrower bandwidth and a higher transmission coefficient compared to the single polarized structure. This can be explained by using the quality factor (Q-factor) equation of the parallel *RLC* circuit which is given by:

$$Q = \frac{\omega}{B} = \omega\, RC \tag{4}$$

where ω is the resonant frequency ($\omega = 2\pi f$). B is the bandwidth and equal to the difference between the two half power frequencies:

$$B = \omega_1 - \omega_2 = \frac{1}{RC} \tag{5}$$

At ω_1 and ω_2 the power on the resistor becomes half of the maximum. The quality factor increases with the increase of C and the bandwidth decreases consequently. As mentioned, increasing the number of layers will shift the resonant frequency downward. The equivalent circuit of this structure is very similar to the single polarised one, taking into consideration that the value of the C_{cc} is halved. Table II shows the variation in the resonant frequency when increasing the number of layers, n. As can be seen from the table, the resonant frequency of the two-layer (n = 2) structure is 1.98 GHz, as shown in Fig. 9. The same dielectric material of FR4 with 0.127 mm thickness is used in the design. The size of the array element is 0.0396λ × 0.0396λ. The resonant frequency of the structure with three metallic layers (n = 3) and two dielectric layers is 1.50 GHz, as shown in Fig. 10. The array element size is 0.03λ × 0.03λ.

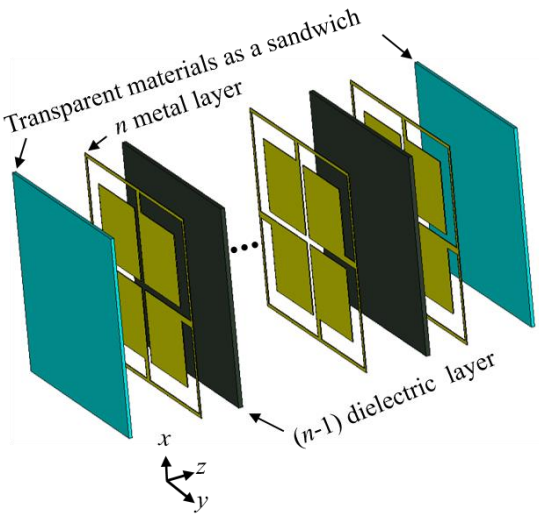

Fig. 8. Structure of the multi-layer bandpass FSS for dual polarizations.

Table II
Element size vs number of metallic layers.

n	f (GHz)	BW	S_{11} (dB)	Overall thickness (mm)	Element size
2	1.96	10.32%	-22.5	0.147	0.038λ
3	1.50	8.42%	-22.0	0.284	0.030λ
4	1.32	6.37%	-19.2	0.421	0.026λ
5	1.21	4.45%	-16.8	0.558	0.024λ

To demonstrate the resonance stability performance for the proposed FSSs with two and three metallic layers, the performance of the FSSs as a function of varied incident angles is shown in Fig. 9 and Fig. 10, respectively. The proposed structures are insensitive to the angle of incidence (θ) up to 75º for both vertical and horizontal polarizations as shown.

The structures were also simulated under various incident angles for the TM mode. The results show that the structures exhibit very stable performance at oblique incident angles as well. For the two-layer structure, the insertion losses are almost the same at 0.396 dB at the normal and 15˚ incident angles. The insertion losses are 0.383 dB at 30˚, 0.347 dB at 45˚, 0.287 dB at 60˚ and 0.117 dB at 75˚, respectively. The resonant frequency is always the same at 1.96 GHz. For the three-layer structure, the insertion loss is 0.645 dB at the normal incident angle. The losses are 0.582 dB at 15˚, 0.515 dB at 30˚, 0.486 dB at 45˚, 0.415 dB at 60˚ and 0.212 dB at 75˚ incident angles. The resonant frequency is the same at 1.5 GHz for all angles.

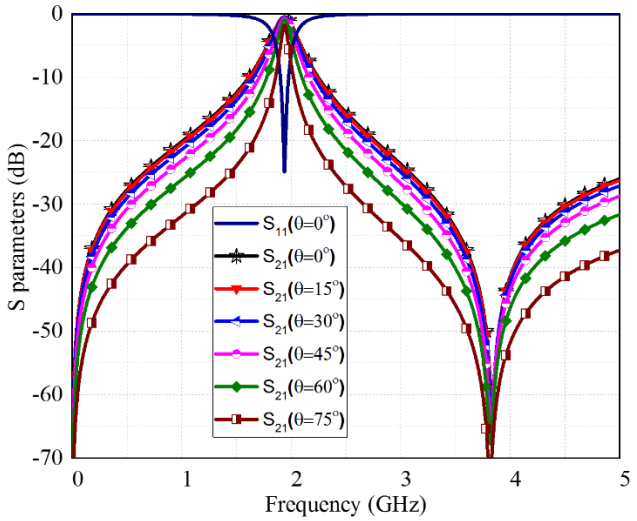

Fig. 9. Simulated frequency responses of the two-metallic-layer FSS (n = 2) under different incident angles. The performance is the same for the vertical and horizontal polarizations.

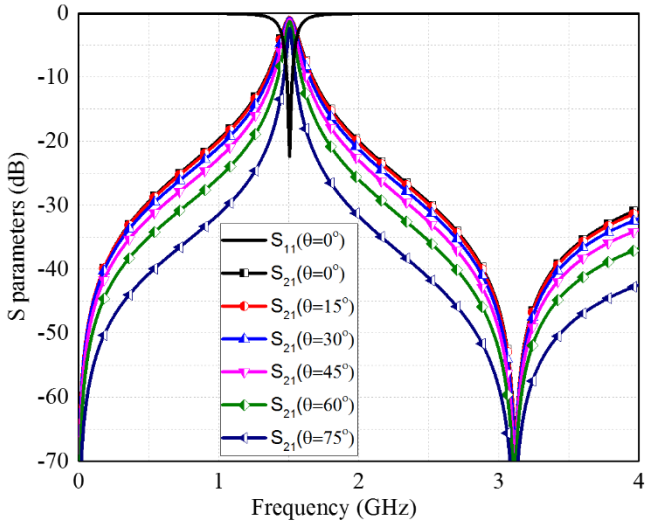

Fig. 10. Simulated frequency responses of the three-metallic-layer FSS (n = 3) under different incident angles. The performance is the same for the vertical and horizontal polarizations.

IV. SURROUNDING DIELECTRIC MATERIALS

The performance of a conventional FSS is affected by dielectric materials attached to it. For a wide range of applications, it is desirable to design FSS structures that can

achieve stable response when the FSS is attached to dielectric materials. The proposed structures here are very stable even though they are attached to dielectric materials of arbitrary thickness on both sides. To understand why the structure is stable compared with traditional structures, it is necessary to understand the effect of the surrounding dielectric material on conventional FSS structures. The main reason is that the resonant components are affected by the surrounding dielectric material, especially the intrinsic capacitance. It can be clearly concluded from (2) that the equivalent intrinsic capacitance of the FSS element depends on the effective dielectric constant ε_e of the structure. The surrounding dielectric directly changes the effective dielectric constant value and thus the capacitance. This can be proven by using a non-resonant FSS structure such as an inductive FSS (highpass) using wires or a capacitive FSS (lowpass or bandstop) using patches. When an inductive FSS structure (wire structure) is attached to a dielectric material, the frequency response is very stable, while the frequency response of the patch type FSS is shifted significantly when the structure is attached to dielectric materials. In traditional FSS structures where both wires and patches are used, the resonant frequency is very sensitive to surrounding dielectric materials.

In the proposed structure, the cross-layer capacitance is introduced and is very strong in the FSS element. This capacitor is not influenced by the surrounding dielectric material, as can be seen from (3). Especially for a low-profile dielectric substrate, the cross-layer capacitor is dominant and diminishes the impact of surrounding materials to the intrinsic capacitance. This makes the resonant frequency very stable against surrounding dielectric materials.

The resonant frequency of the proposed structure, by ignoring the intrinsic capacitor, can be obtained by:

$$f = \frac{1}{2\pi\sqrt{LC}} \tag{6}$$

The values of L and C can be obtained from (1) and (3). The resonant frequency can be obtained by:

$$f = \frac{c}{\sqrt{2\pi P \frac{(n-1)}{n} \log\left(\frac{1}{\sin\frac{\pi w}{2P}}\right)\left(\frac{\varepsilon_r A}{d}\right)}} \tag{7}$$

where A is equal to $2(a\times b)$ in the single polarized case and $2a^2$ for the dual polarized structure, c is the velocity of light, and n is the number of metallic layers.

To demonstrate this feature of the proposed design, the structure with dielectric materials attached is simulated using CST. Fig. 11 shows the comparison of frequency responses of the proposed structure shown in Fig. 8 with $n = 2$ in three cases: without any attaching dielectric material, with a dielectric material attached to one side and with a dielectric material attached to both sides of the structure. The dielectric material is a 1.6 mm thick FR4. It can be seen that the resonant frequency is only shifted by 3.7% when the dielectric material is attached to one side, and shifted by 6.7% when the dielectric material is attached to both sides. Fig. 12 shows the comparison of this structure in the case of $n = 3$. In this case, the resonant frequency is only shifted by 1.5% when the dielectric material is attached to one side, and shifted by 3.4% when the dielectric material is attached to both sides.

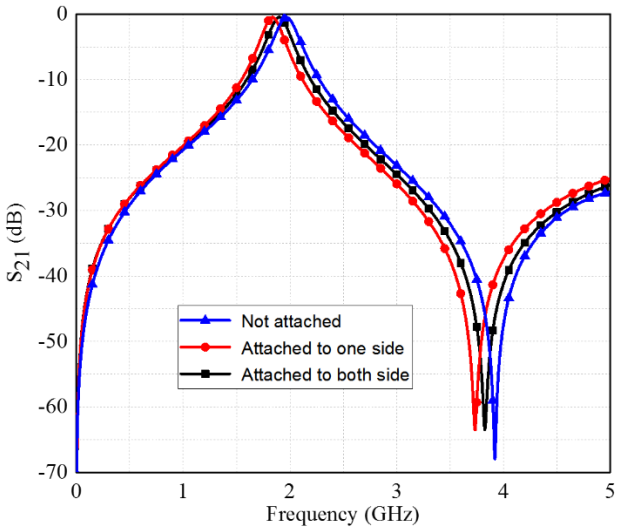

Fig. 11. Simulated frequency responses of the two-metallic-layer FSS (n=2) with or without surrounding dielectric materials attached to the FSS.

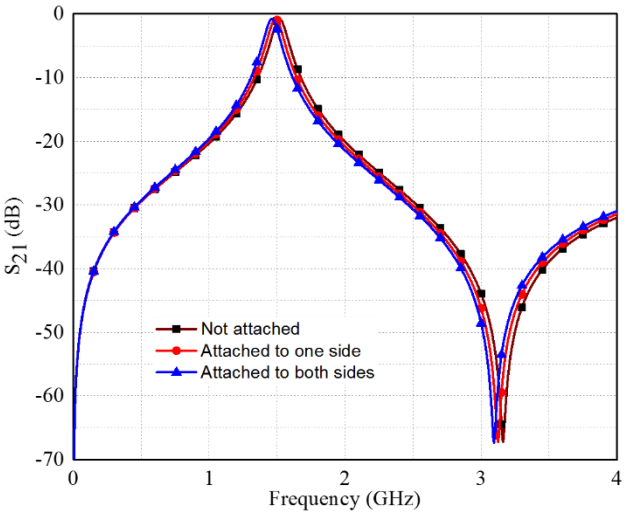

Fig. 12. Simulated frequency responses of the three-metallic-layer FSS (n = 3) with or without surrounding dielectric materials attached to the FSS.

It should be noted that the advantages of the proposed design were achieved mainly because the proposed structure on any layer is not symmetrical by itself along either the x-axis or the y-axis. The metallic layout in one layer is the flipped, or anti-parallel, version of the layout in the adjacent layer. This arrangement dramatically strengthens the cross-layer capacitance. The cross-layer capacitance makes the structure not only small, but also insensitive to surrounding dielectric materials. In contrast, in traditional FSSs, the structures in each layer are parallel to each other. The current and charge distributions on each side are the same. There is no strong capacitance between adjacent layers. To prove this, a patch-mesh FSS structure, as shown in Fig.13(a), is used as an

example to show the effect of surrounding dielectric materials on traditional FSSs.

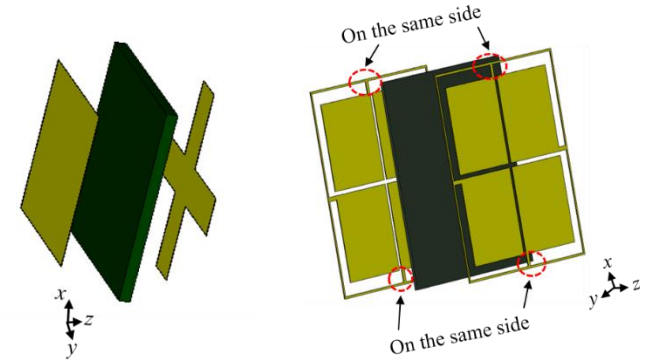

(a) (b)

Fig. 13. Traditional FSS structures as examples to demonstrate the effect of surrounding dielectric materials on the FSS's response, (a) patch-mesh structure, (b) proposed structure with identical metallic structures on adjacent layers but not flipped.

In Fig. 13(b), the proposed structure without flipping the shape of the bottom layer is used as another example to prove the advantage of the proposed design. To make comparison more logical, the dimensions are tuned to achieve similar resonant frequencies to the proposed structure. The substrate between metallic layers in these examples is an FR4 with a thickness of 0.127 mm.

First of all, the array element dimensions of these two examples are much bigger than the proposed one. The periodic dimension of the patch-mesh structure is 0.22λ, and it is 0.13λ for the example in Fig. 13 (b). The periodic dimension of the proposed FSS element is only 0.012λ as shown in Table I. The dimension of the proposed FSS element is more than 18 times smaller than the traditional patch-mesh structure and the area is 330 times smaller.

Table III
The normalised resonant frequency deviation when the structures are attached to an FR4 dielectric substrate with different thicknesses. t is the thickness of surrounding dielectric materials. The results are obtained by simulation.

The structures	Attached to one side		Attached to both sides	
	Dev (t=1.6mm)	Dev (t=3mm)	Dev (t=1.6mm)	Dev (t=3mm)
The patch-mesh structure (Fig. 13(a))	0.21	0.26	0.26	0.33
The proposed structure without C_{cc} (Fig.13(b))	0.28	0.31	0.36	0.43
The proposed structure (n=2)	0.037	0.045	0.065	0.080
The proposed structure (n=3)	0.015	0.021	0.034	0.062
The proposed structure (n=4)	0.011	0.015	0.024	0.03

Table III compares the performance of the proposed dual-polarized structure with the two traditional FSS structures shown in Fig. 13. The normalised deviation (Dev) is defined as the difference between the resonant frequency of each structure before being attached to the dielectric material (f) and the resonant frequency after being attached to the dielectric (f_d) divided by f. That is, Dev = (f- f_d)/ f. It can be seen that the insensitivity of the proposed structure is about six times better than traditional structures. The cases where they are attached to a higher dielectric constant material (ε_r = 8) is compared in Table IV.

It should be noted that in [21] the circuit element was also miniaturized by a cross-layer capacitance. However the structure is still relatively sensitive to surrounding materials compared to the proposed structure. It was found by simulation that the proposed structure is two to three times less sensitive than the one in [21]. The main reason is that the proposed structure has a much lower intrinsic capacitance and a stronger cross-layer capacitance due to the charge distribution as analysed in Fig. 2.

Table IV
The normalised resonant frequency deviation obtained by simulation when the structure are attached to a higher dielectric constant material, ε_r = 8.

The structures	Attached to one side		Attached to both sides	
	Dev (t = 1.6mm)	Dev (t = 3mm)	Dev (t = 1.6mm)	Dev (t = 3mm)
The patch-mesh structure (Fig. 13(a))	0.27	0.33	0.36	0.41
The proposed structure without C_{cc} (Fig.13(b))	0.37	0.44	0.51	0.56
The proposed structure (n=2)	0.065	0.077	0.122	0.148
The proposed structure (n=3)	0.039	0.047	0.073	0.089
The proposed structure (n=4)	0.024	0.038	0.051	0.063

It is clearly shown that the proposed structure exhibit very stable performance compared with traditional FSSs. Increasing the number of metallic layers contributes to making the resonant frequency of the proposed structure even more stable, as shown in these tables. The resonant frequency of a four-layer structure is about 2.5 times more stable than a two-layer one. This is mainly due to that much stronger cross-layer capacitance will be induced in multi-layer (n > 2) structures, while the intrinsic capacitance is affected the same way as the two-layer structure.

V. Experimental Results

A prototype of the proposed FSS as shown in Fig. 8 has been fabricated and measured to validate the design. The fabricated FSS is shown in Fig. 14. The size of the FSS prototype is 180 mm × 180 mm and it consists of 30 × 30 elements.

Two horn antennas and a vector network analyzer were used for the measurement. The measurement setup is shown in Fig. 15. The line of sight between the two antennas passes through the centre of the FSS prototype and the antennas are located about 70 cm away from the fixture to ensure the formation of uniform plane wave impinging upon the FSS structure. When carrying out the measurement at 60˚, the absorbers at the side were adjusted so as not to block the incident wave. Measurement of the fabricated FSS is performed in two steps. Firstly, the transmission response of the system without the FSS is measured. This measurement result is used to calibrate the FSS response. Secondly, the frequency response with the presence of the FSS structure is measured.

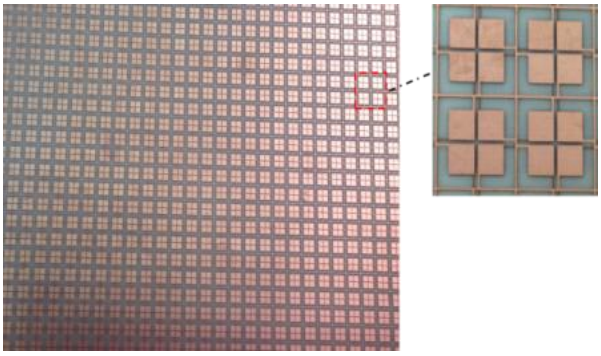

Fig. 14. Photograph of the prototype of the proposed FSS with n = 2.

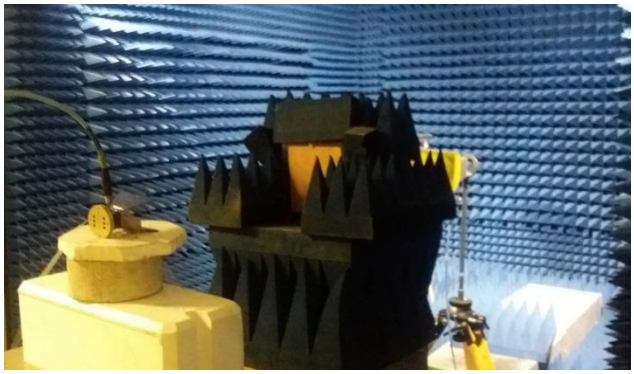

Fig. 15. Measurement setup to measure the transmission coefficient of the FSS.

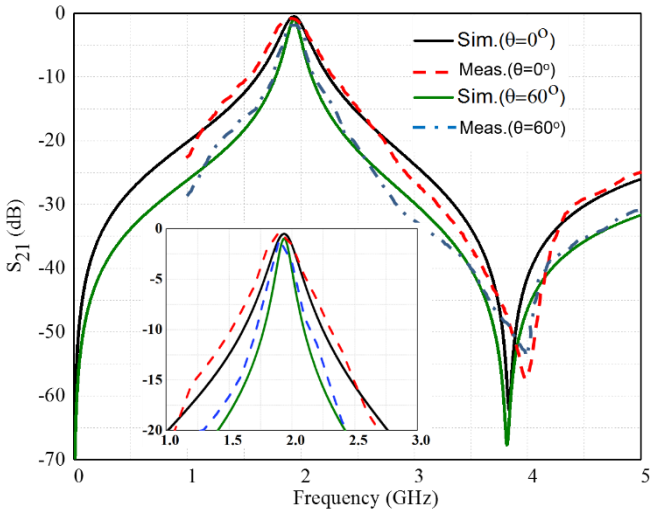

Fig. 16. Measured and simulated frequency responses of the two-metallic-layer (n = 2) FSS under different incident angles.

In the example of the FSS with two metallic layers (n = 2), the fabrication is performed by patterning the proposed shape on two sides of a 0.127 mm thick FR4 substrate. The measured performances with incident angles of 0° and 60° for this prototype are shown in Fig. 16. The measured insertion loss is 0.73 dB at the resonant frequency for normal incidence, which is mainly attributed to the dielectric and the metallic losses of the structure. The measured performance is compared with the simulated one. It can be seen that very good agreement has been achieved. The transmission with other incident angles up to 75° was also measured. The measured performance is also in very good agreement with the simulated one. Such results are not shown in this figure to avoid having too many curves in the figure.

To measure reflection, the two horn antennas are used as the transmitter and receiver, respectively, at the same side of the FSS. They are separated by an absorber screen to eliminate the direct coupling between them. The measured reflection of the prototype of the proposed FSS is shown in Fig. 17. The measured result is in very good agreement with the simulated performance.

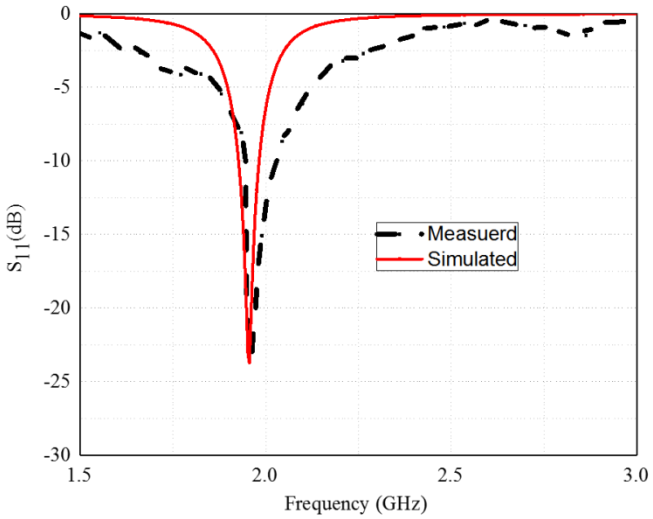

Fig. 17. Measured and simulated reflection coefficients of the two-metallic-layer (n = 2) FSS.

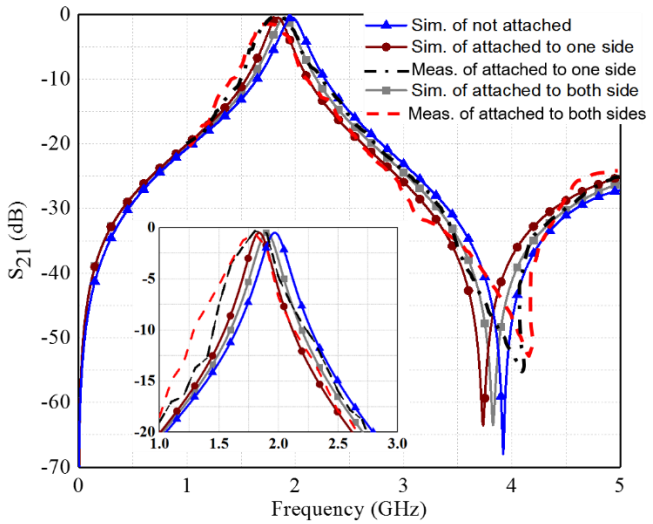

Fig. 18. Measured and simulated frequency responses of the two metallic layers FSS (n = 2) with or without surrounding dielectric materials.

A 1.6 mm thick FR4 dielectric material is attached to the prototype of the structure with n = 2. The dielectric material is firstly attached to one side of the structure and then attached to both sides. The transmission coefficients were measured and shown in Fig. 18, to prove the stability of the proposed structure when it is attached directly to dielectric materials. It can be seen that the resonant frequency is shifted about 4.0% when the dielectric material is attached to one side, and about 6.9% when

attached to both sides. The measured results are in good agreement with the simulated ones as summarized in Table III.

In the example with three metallic layers (n = 3), the fabrication is performed by firstly patterning the proposed two-metallic-layer structure on a 0.127 mm thick FR4 substrate. The third metallic layer is patterned on one side of another FR4 substrate while etching away the copper cladding on the other side. The two PCBs are then compressed together by using a transparent material (lastre Polycarbonates lexan), with a dielectric constant of 2.9, in a sandwich structure. This transparent material caused very little change to the frequency response. The effect of the supporting material is taken into account in the simulation. The alignment between adjacent layers is very important to achieve good performance. The measured performances with an incident angle of 0° and 60° for this prototype are shown in Fig. 19. The measured insertion loss is about 0.87 dB at its resonant frequency for normal incidence.

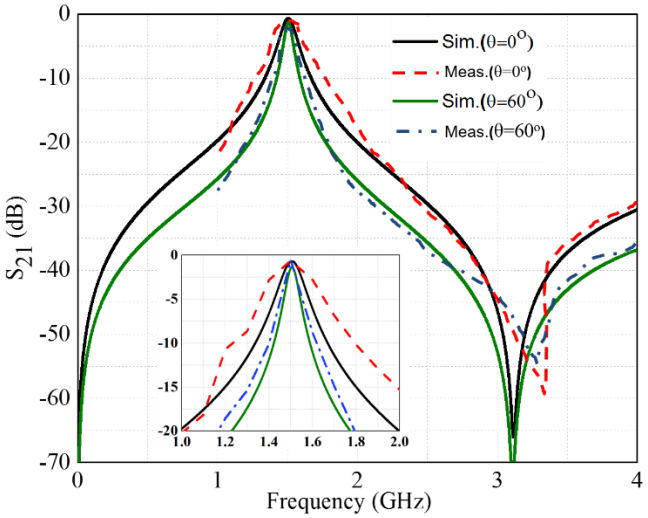

Fig. 19. Measured and simulated frequency responses of the three-metallic-layer FSS (n = 3) under different incident angles.

A 1.6 mm thick FR4 dielectric material was attached to the prototype. Similarly, the dielectric material is firstly attached to one side of the prototype and then to both sides. The transmission coefficient is measured as shown in Fig. 20. It can be seen that the resonant frequency is shifted by about 1.5% when the dielectric material is attached to one side and by 3.4% when attached to both sides. The measured results are in good agreement with the simulated one as summarized in Table III. Very good agreement between simulation and measurement has been achieved.

The measured results of the miniaturized FSSs show that the resonant frequency is shifted downward from 1.96 GHz to 1.52 GHz by increasing n from 2 to 3. They are also in good agreement with the simulation. This confirms that the proposed structure acts as a miniaturized low profile bandpass FSS and it is insensitive to surrounding dielectric materials.

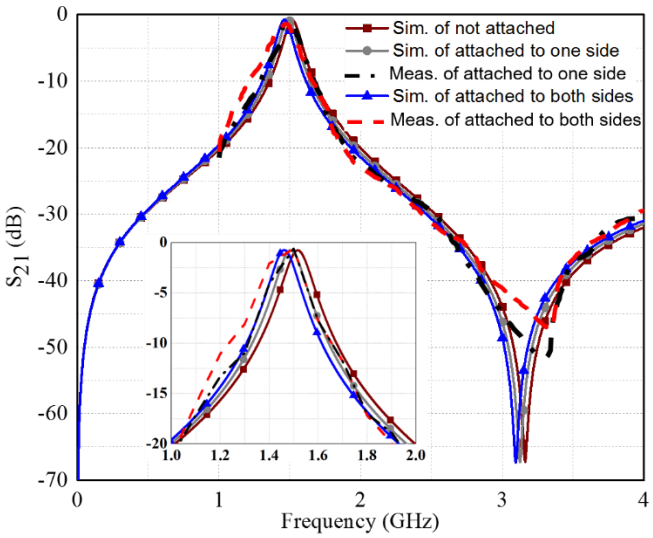

Fig. 20. Measured and simulated frequency responses of the three-metallic-layer FSS (n = 3) with or without surrounding dielectric materials.

VI. Conclusion

An unconventional approach has been proposed to design miniaturized multi-layer FSS structures in this paper. The proposed bandpass FSS exhibits a very stable frequency response when it is attached to dielectric materials of arbitrary thicknesses, about six times better than conventional FSS structures.

The overall thicknesses of the multi-layer FSSs presented in this paper are extremely small. As an example, the thickness of the FSS structure consisting of three metallic layers and two dielectric layers is less than 0.5 mm. Unlike traditional structures, the size of the proposed FSS element is smaller when the profile is lower.

The dimensions of the miniaturized element are much smaller than the wavelength at the resonant frequency, as small as $0.012\lambda \times 0.012\lambda$ which is one of the smallest reported so far. For a two-metallic-layer structure, the size of the proposed dual polarized FSS element is 330 times smaller than the traditional patch-mesh structure.

The proposed approach to design miniaturized FSSs was experimentally verified by two prototypes. The simulation and measurement results verify the stable frequency response of the proposed design. These advantages of the proposed structure can be useful for many applications where circuit compactness, having a low profile and insensitivity to surrounding materials are desired.

References

[1] G. Schennum, "Frequency-selective surfaces for multiple-frequency antennas," *Microw. J.*, vol. 16, pp. 55-57, 1973.

[2] Y. Rahmat-Samii, and M. Gatti, "Far-field patterns of spaceborne antennas from plane-polar near-field measurements," *IEEE Trans. Antennas Propag.*, vol. 33, no. 6, pp. 638-648, Jun. 1985.

[3] Y. Rahmat-Samii, and A. N. Tulintseff, "Diffraction analysis of frequency selective reflector antennas," *IEEE Trans. Antennas Propag.*, vol. 41, no. 4, pp. 476-487, Apr. 1993.

[4] T. K. Wu, "Cassini Frequency-Selective Surface Development," *J. Electromagn. Waves Applicat.*, vol. 8, no. 12, pp. 1547-1561, 1994.
[5] R. Ott, R. Kouyoumjian, and L. Peters, "Scattering by a Two-Dimensional Periodic Array of Narrow Plate," *Radio Science*, vol. 2, no. 11, pp. 1347-1359, Nov. 1967.
[6] B. Munk, and R. Luebbers, "Reflection properties of two-layer dipole arrays," *IEEE Trans. Antennas Propag.*, vol. 22, no. 6, pp. 766-773, Nov. 1974.
[7] C. Winnewisser, F. Lewen, and H. Helm, "Transmission characteristics of dichroic filters measured by THz time-domain spectroscopy," *Appl. Phys. A*, vol. 66, no. 6, pp. 593-598, Jun. 1998.
[8] S. Govindaswamy, J. East, F. Terry, E. Topsakal, J. L. Volakis, and G. I. Haddad, "Frequency-selective surface based bandpass filters in the near-infrared region," *Microw. Opt. Technol. Lett.*, vol. 41, no. 4, pp. 266-269, May 2004.
[9] R. Ulrich, "Far-Infrared Properties of Metallic Mesh and Its Complementary Structure," *Infrared Phys.*, vol. 7, no. 1, pp. 37-&, 1967.
[10] F. Bayatpur, and K. Sarabandi, "Single-layer high-order miniaturized-element frequency-selective surfaces," *IEEE Trans. Microw. Theory Techn.* , vol. 56, no. 4, pp. 774-781, Apr. 2008.
[11] B. Schoenlinner, A. Abbaspour-Tamijani, L. C. Kempel, and G. M. Rebeiz, "Switchable low-loss RF MEMS Ka-band frequency-selective surface," *IEEE Trans. Microw. Theory Techn.*, vol. 52, no. 11, pp. 2474-2481, Nov. 2004.
[12] D. Sievenpiper, L. J. Zhang, R. F. J. Broas, N. G. Alexopolous, and E. Yablonovitch, "High-impedance electromagnetic surfaces with a forbidden frequency band," *IEEE Trans. Microw. Theory Techn.*, vol. 47, no. 11, pp. 2059-2074, Nov. 1999.
[13] B. A. Munk, *Frequency selective surfaces*: *Theory and Design*. New York: john Wiley&Sons, Wiley-Interscience, 2000.
[14] F. C. Huang, C. N. Chiu, T. L. Wu, and Y. P. Chiou, "A Circular-Ring Miniaturized-Element Metasurface With Many Good Features for Frequency Selective Shielding Applications," *IEEE Trans. Electromagn. Compa.*, vol. 57, no. 3, pp. 365-374, Jun. 2015.
[15] S. N. Azemi, K. Ghorbani, and W. S. T. Rowe, "Angularly Stable Frequency Selective Surface With Miniaturized Unit Cell," *IEEE Microw. Compon. Lett.*, vol. 25, no. 7, pp. 454-456, Jul. 2015.
[16] G. H. Yang, T. Zhang, W. L. Li, and Q. Wu, "A Novel Stable Miniaturized Frequency Selective Surface,"*IEEE Antennas Wireless Propag. Lett.* vol. 9, pp. 1018-1021, Oct. 2010.
[17] C. N. Chiu, and K. P. Chang, "A Novel Miniaturized-Element Frequency Selective Surface Having a Stable Resonance,"IEEE Antennas Wireless Propag. Lett. vol. 8, pp. 1175-1177, Oct. 2009.
[18] K. Sarabandi, and N. Behdad, "A frequency selective surface with miniaturized elements," *IEEE Trans. Antennas Propag.*, vol. 55, no. 5, pp. 1239-1245, May 2007.
[19] H. Liu, K. L. Ford, and R. J. Langley, "Miniaturised bandpass frequency selective surface with lumped components," *Electron. Lett.*, vol. 44, no. 18, pp. 1054-U12, Aug. 2008.
[20] S. Sheikh, "Miniaturized-Element Frequency-Selective Surfaces Based on the Transparent Element to a Specific Polarization," *IEEE Antennas Wireless Propag. Lett*, vol. 15, pp. 1661-1664, Jan. 2016.
[21] B.-Q. Lin, S.-H. Zhou, X.-Y. Da, Y.-W. Fang, Y.-J. Li, and W. Li, "Compact miniaturised-element frequency selective surface," *Electron. Lett.*, vol. 51, no. 12, pp. 883-884, Jun. 2015.
[22] J. Lorenzo, A. Lázaro, R. Villarino, and D. Girbau, "Modulated frequency selective surfaces for wearable RFID and sensor applications," *IEEE Trans. Antennas Propag.*, vol. 64, no. 10, pp. 4447-4456, Aug. 2016.
[23] D. M. Dobkin, and S. M. Weigand, "Environmental effects on RFID tag antennas," *2005 IEEE MTT-S International Microwave Symposium Digest*, 2005, pp. 135-138.
[24] S. Shao, R. J. Burkholder, and J. L. Volakis, "Design Approach for Robust UHF RFID Tag Antennas Mounted on a Plurality of Dielectric Surfaces," *IEEE Antennas Propag. Mag.* , vol. 56, no. 5, pp. 158-166, Oct. 2014.
[25] N. Marcuvitz, *Waveguide handbook*: Iet, 1951.
[26] M. Al-Joumayly, and N. Behdad, "A new technique for design of low-profile, second-order, bandpass frequency selective surfaces," *IEEE Trans. Antennas Propag.*, vol. 57, no. 2, pp. 452-459, 2009.

MUAAD NASER HUSSEIN was born in Basra, Iraq. He received the B.Sc. and M.Sc. degrees in electrical engineering from the University of Basra, Iraq, in 2005. He is currently pursuing the Ph.D. degree in electrical engineering and electronics with the University of Liverpool, U.K. He was a Microwave Engineer with ASIACELL Telecom., Sulaimaniyah, Iraq, for seven years. He has been a Lecturer with the Department of Electrical Power Engineering, South Technical University, Basra, Iraq. His research interests focus on frequency selective surfaces, wireless power transfer, and antenna design.

Jiafeng Zhou received a B.Sc. degree in Radio Physics from Nanjing University, Nanjing, China, in 1997, and a Ph.D. degree from the University of Birmingham, Birmingham, U.K., in 2004. His doctoral research concerned high-temperature superconductor microwave filters.

From July 1997, for two and a half years he was with the National Meteorological Satellite Centre of China, Beijing, China, where he was involved with the development of communication systems for Chinese geostationary meteorological satellites. From August 2004 to April 2006, he was a Research Fellow with the University of Birmingham, where his research concerned phased arrays for reflector observing systems. Then he moved to the Department of Electronic and Electrical Engineering, University of Bristol, Bristol, U.K until August 2013. His research in Bristol was on the development of highly efficient and linear amplifiers. He is now with the Department of Electrical Engineering and Electronics, University of Liverpool, Liverpool, UK. His current research interests include microwave power amplifiers, filters, electromagnetic energy harvesting and wireless power transfer.

Yi Huang (S'91 – M'96 – SM'06) received BSc in Physics (Wuhan University, China) in 1984, MSc (Eng) in Microwave Engineering (NRIET, Nanjing, China) in 1987, and DPhil in Communications from the University of Oxford, UK in 1994.

He has been conducting research in the areas of wireless communications, applied electromagnetics, radar and antennas since 1987. His experience includes 3 years spent with NRIET (China) as a *Radar Engineer* and various periods with the Universities of Birmingham, Oxford, and Essex at the UK as a member of research staff. He worked as a *Research Fellow* at British Telecom Labs in 1994, and then joined the Department of Electrical Engineering & Electronics, the University of Liverpool, UK as a *Faculty* in 1995, where he is now a full *Professor in Wireless Engineering*, the *Head of High Frequency Engineering Group and Deputy Head of Department*.

Prof Huang has published over 300 refereed papers in leading international journals and conference proceedings, and authored *Antennas: from Theory to Practice* (John Wiley, 2008) and *Reverberation Chambers: Theory and Applications to EMC and Antenna Measurements* (John Wiley, 2016). He has received many research grants from research councils, government agencies, charity, EU and industry, acted as a consultant to various companies, and served on a number of national and international technical committees and been an *Editor, Associate Editor or Guest Editor* of four of international journals. He has been a *keynote/invited speaker* and *organiser* of many conferences and workshops (e.g. WiCom 2006, 2010, IEEE iWAT2010, and LAPC2012). He is at present the *Editor-in-Chief* of Wireless Engineering and Technology, *Associate Editor* of IEEE Antennas and Wireless Propagation Letters, *UK and Ireland Rep* to European Association of Antenna and Propagation (EurAAP), a *Senior Member* of IEEE, *Senior Fellow* of HEA, and a *Fellow* of IET.

Muayad Kod received the B.Sc. and M.Sc. degrees from the Department of Electronics and Communications, Al-Nahrain University, Baghdad, Iraq, in 2002 and 2005, respectively. He received the Ph.D. degree from the Department of Electrical Engineering and Electronics, The University of Liverpool, Liverpool, U.K, in 2016.

He was an OMC Engineer with Global Telecom Holding/Iraqna, Baghdad, Iraq, in 2005. In 2007, he joined Asiacell, Sulaimaniyah, Iraq, as a Radio Frequency (RF) Engineer, where he was involved in telecommunication, and moved to Omnnea, Najaf, Iraq, as an RF Engineering Team Leader in 2008, where he was involved in wireless telecommunications. Since 2009, he has been a Lecturer with the Department of Electrical Engineering and Electronics, University of Kerbala, Karbala, Iraq. His current research interests include wireless power transfer and telemetry to implantable medical devices, wearable and implantable antennas, RFID, energy harvesting and frequency selective surfaces.

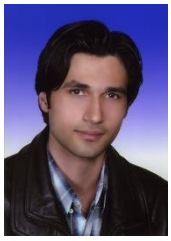

Abed Pour Sohrab was born in Bandar Anzali, Iran. He received the BSc degree in electrical engineering from K. N. Toosi University of Technology, Tehran, Iran, in 2008 and the MSc degree in electromagnetics and antenna engineering from Tarbiat Modares University, Tehran, Iran, in 2012. He is currently pursuing the PhD degree in electrical engineering at University of Liverpool, UK. His research interests include frequency selective surfaces, electromagnetic absorbers, UHF RFID tags and novel antenna designing.